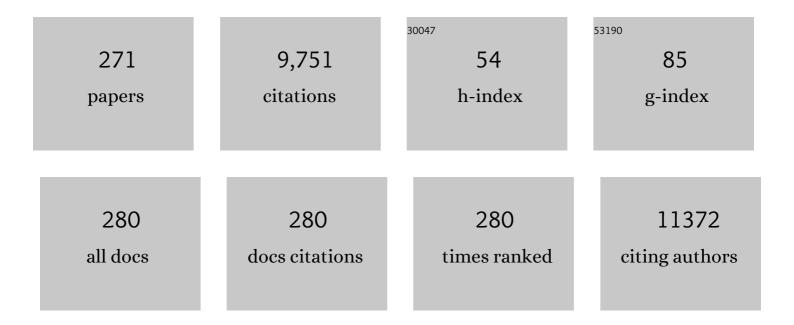
Stephen D Evans

List of Publications by Year in descending order

Source: https://exaly.com/author-pdf/1601383/publications.pdf Version: 2024-02-01



#	Article	IF	CITATIONS
1	Controlling the Optical Properties of Gold Nanorods in One-Pot Syntheses. Journal of Physical Chemistry C, 2022, 126, 3235-3243.	1.5	9
2	An Open Access Chamber Designed for the Acoustic Characterisation of Microbubbles. Applied Sciences (Switzerland), 2022, 12, 1818.	1.3	2
3	Chiral nematic liquid crystal droplets as a basis for sensor systems. Molecular Systems Design and Engineering, 2022, 7, 607-621.	1.7	15
4	Receptor tyrosine kinases regulate signal transduction through a liquid-liquid phase separated state. Molecular Cell, 2022, 82, 1089-1106.e12.	4.5	38
5	A Single Short â€~Tone Burst' Results in Optimal Drug Delivery to Tumours Using Ultrasound-Triggered Therapeutic Microbubbles. Pharmaceutics, 2022, 14, 622.	2.0	6
6	Modeling the mechanical stiffness of pancreatic ductal adenocarcinoma. Matrix Biology Plus, 2022, 14, 100109.	1.9	7
7	Mechanically tuneable physical nanocomposite hydrogels from polyelectrolyte complex templated silica nanoparticles for anionic therapeutic delivery. Journal of Colloid and Interface Science, 2022, 617, 224-235.	5.0	11
8	Protein-conjugated microbubbles for the selective targeting of S. aureus biofilms. Biofilm, 2022, 4, 100074.	1.5	5
9	Developing a Raman spectroscopy-based tool to stratify patient response to pre-operative radiotherapy in rectal cancer. Analyst, The, 2021, 146, 581-589.	1.7	9
10	Polyelectrolyte complex templated synthesis of monodisperse, sub-100Ânm porous silica nanoparticles for cancer targeted and stimuli-responsive drug delivery. Journal of Colloid and Interface Science, 2021, 584, 669-683.	5.0	11
11	Novel oxygen-generation from electrospun nanofibrous scaffolds with anticancer properties: synthesis of PMMA-conjugate PVP–H ₂ O ₂ nanofibers, characterization, and <i>in vitro</i> bio-evaluation tests. RSC Advances, 2021, 11, 19978-19991.	1.7	8
12	Production of giant unilamellar vesicles and encapsulation of lyotropic nematic liquid crystals. Soft Matter, 2021, 17, 2234-2241.	1.2	15
13	Model Lipid Membranes Assembled from Natural Plant Thylakoids into 2D Microarray Patterns as a Platform to Assess the Organization and Photophysics of Lightâ€Harvesting Proteins. Small, 2021, 17, e2006608.	5.2	7
14	Evaluating Phospholipidâ€Functionalized Gold Nanorods for In Vivo Applications. Small, 2021, 17, 2006797.	5.2	14
15	10.1063/5.0040213.1.,2021,,.		0
16	Horizon: Microfluidic platform for the production of therapeutic microbubbles and nanobubbles. Review of Scientific Instruments, 2021, 92, 074105.	0.6	15
17	Targeted microbubbles carrying lipid-oil-nanodroplets for ultrasound-triggered delivery of the hydrophobic drug, combretastatin A4. Nanomedicine: Nanotechnology, Biology, and Medicine, 2021, 36, 102401.	1.7	10
18	Nanobubbles for therapeutic delivery: Production, stability and current prospects. Current Opinion in Colloid and Interface Science, 2021, 54, 101456.	3.4	29

#	Article	IF	CITATIONS
19	Synthesis of near-infrared absorbing triangular Au nanoplates using biomineralisation peptides. Acta Biomaterialia, 2021, 131, 519-531.	4.1	7
20	Textures of Nematic Liquid Crystal Cylindric-Section Droplets Confined by Chemically Patterned Surfaces. Crystals, 2021, 11, 65.	1.0	5
21	Mercaptopurine-Loaded Sandwiched Tri-Layered Composed of Electrospun Polycaprolactone/Poly(Methyl Methacrylate) Nanofibrous Scaffolds as Anticancer Carrier with Antimicrobial and Antibiotic Features: Sandwich Configuration Nanofibers, Release Study and in vitro Bioevaluation Tests. International Journal of Nanomedicine. 2021. Volume 16. 6937-6955.	3.3	15
22	Ultrasound-triggered therapeutic microbubbles enhance the efficacy of cytotoxic drugs by increasing circulation and tumor drug accumulation and limiting bioavailability and toxicity in normal tissues. Theranostics, 2020, 10, 10973-10992.	4.6	45
23	Oneâ€Step Preparation of Biocompatible Gold Nanoplates with Controlled Thickness and Adjustable Optical Properties for Plasmonâ€Based Applications. Advanced Functional Materials, 2020, 30, 2003512.	7.8	22
24	Site-directed M2 proton channel inhibitors enable synergistic combination therapy for rimantadine-resistant pandemic influenza. PLoS Pathogens, 2020, 16, e1008716.	2.1	9
25	Exploring High Aspect Ratio Gold Nanotubes as Cytosolic Agents: Structural Engineering and Uptake into Mesothelioma Cells. Small, 2020, 16, e2003793.	5.2	7
26	Freeze-Dried Therapeutic Microbubbles: Stability and Gas Exchange. ACS Applied Bio Materials, 2020, 3, 7840-7848.	2.3	6
27	Detection and time-tracking activation of a photosensitiser on live single colorectal cancer cells using Raman spectroscopy. Analyst, The, 2020, 145, 5878-5888.	1.7	10
28	Control of Director Fields in Phospholipid-Coated Liquid Crystal Droplets. Langmuir, 2020, 36, 6436-6446.	1.6	20
29	Nested Nanobubbles for Ultrasound-Triggered Drug Release. ACS Applied Materials & Interfaces, 2020, 12, 29085-29093.	4.0	27
30	High-throughput microfluidics for evaluating microbubble enhanced delivery of cancer therapeutics in spheroid cultures. Journal of Controlled Release, 2020, 326, 13-24.	4.8	38
31	Out-of-Plane Nanoscale Reorganization of Lipid Molecules and Nanoparticles Revealed by Plasmonic Spectroscopy. Journal of Physical Chemistry Letters, 2020, 11, 2875-2882.	2.1	3
32	Screening and characterisation of CdTe/CdS quantum dot-binding peptides for material surface functionalisation. RSC Advances, 2020, 10, 8218-8223.	1.7	4
33	Rotatable microfluidic device for simultaneous study of bilateral chemosensory neurons in Caenorhabditis elegans. Microfluidics and Nanofluidics, 2020, 24, 1.	1.0	4
34	Physical Biomarkers of Disease Progression: On-Chip Monitoring of Changes in Mechanobiology of Colorectal Cancer Cells. Scientific Reports, 2020, 10, 3254.	1.6	15
35	Dynamic Nanoscale Reorganization of Lipid Molecules and Nanoparticles Revealed by Plasmonic GAP Resonance Spectroscopy. Biophysical Journal, 2020, 118, 87a.	0.2	0
36	A bioinspired peptide matrix for the detection of 2,4,6-trinitrotoluene (TNT). Biosensors and Bioelectronics, 2020, 153, 112030.	5.3	21

#	Article	IF	CITATIONS
37	Nanoparticle-Loaded Hydrogel for the Light-Activated Release and Photothermal Enhancement of Antimicrobial Peptides. ACS Applied Materials & amp; Interfaces, 2020, 12, 24544-24554.	4.0	79
38	Peptide-Functionalized Quantum Dots for Rapid Label-Free Sensing of 2,4,6-Trinitrotoluene. Bioconjugate Chemistry, 2020, 31, 1400-1407.	1.8	16
39	On-chip pressure measurements and channel deformation after oil absorption. SN Applied Sciences, 2020, 2, 1.	1.5	6
40	Organ on chip models for the evaluation of microbubble based therapeutic delivery. , 2020, , .		0
41	Title is missing!. , 2020, 16, e1008716.		Ο
42	Title is missing!. , 2020, 16, e1008716.		0
43	Title is missing!. , 2020, 16, e1008716.		Ο
44	Title is missing!. , 2020, 16, e1008716.		0
45	Title is missing!. , 2020, 16, e1008716.		Ο
46	Title is missing!. , 2020, 16, e1008716.		0
47	Rational screening of biomineralisation peptides for colour-selected one-pot gold nanoparticle syntheses. Nanoscale Advances, 2019, 1, 71-75.	2.2	13
48	Subâ€Nanometer Thick Gold Nanosheets as Highly Efficient Catalysts. Advanced Science, 2019, 6, 1900911.	5.6	56
49	Subâ€Nanometer Thick Gold Nanosheets: Subâ€Nanometer Thick Gold Nanosheets as Highly Efficient Catalysts (Adv. Sci. 21/2019). Advanced Science, 2019, 6, 1970129.	5.6	Ο
50	Molecular Effects of Glycerol on Lipid Monolayers at the Gas–Liquid Interface: Impact on Microbubble Physical and Mechanical Properties. Langmuir, 2019, 35, 10097-10105.	1.6	24
51	Cells Under Stress: An Inertial-Shear Microfluidic Determination of Cell Behavior. Biophysical Journal, 2019, 116, 1127-1135.	0.2	68
52	Developing gold nanotubes as photoacoustic contrast agents. Journal of Physics: Conference Series, 2019, 1151, 012018.	0.3	8
53	Lipid coated liquid crystal droplets for the on-chip detection of antimicrobial peptides. Lab on A Chip, 2019, 19, 1082-1089.	3.1	65
54	Combined flow-focus and self-assembly routes for the formation of lipid stabilized oil-shelled microbubbles. Microsystems and Nanoengineering, 2018, 4, .	3.4	11

#	Article	IF	CITATIONS
55	Confined Assembly of Hollow Carbon Spheres in Carbonaceous Nanotube: A Spheresâ€inâ€Tube Carbon Nanostructure with Hierarchical Porosity for Highâ€Performance Supercapacitor. Small, 2018, 14, e1704015.	5.2	64
56	Morphological control of seedlessly-synthesized gold nanorods using binary surfactants. Nanotechnology, 2018, 29, 135601.	1.3	18
57	Tandem fluorescence and Raman (fluoRaman) characterisation of a novel photosensitiser in colorectal cancer cell line SW480. Analyst, The, 2018, 143, 6113-6120.	1.7	13
58	Developing Hollow-Channel Gold Nanoflowers as Trimodal Intracellular Nanoprobes. International Journal of Molecular Sciences, 2018, 19, 2327.	1.8	8
59	Stimuliâ€Responsive Release of Antimicrobials Using Hybrid Inorganic Nanoparticleâ€Associated Drugâ€Delivery Systems. Macromolecular Bioscience, 2018, 18, e1800207.	2.1	48
60	Recommendations for clinical translation of nanoparticle-enhanced radiotherapy. British Journal of Radiology, 2018, 91, 20180325.	1.0	12
61	Visualization of diffusion limited antimicrobial peptide attack on supported lipid membranes. Soft Matter, 2018, 14, 6146-6154.	1.2	27
62	Enhanced Tubulation of Liposome Containing Cardiolipin by MamY Protein from Magnetotactic Bacteria. Biotechnology Journal, 2018, 13, 1800087.	1.8	12
63	Biochemical fingerprint of colorectal cancer cell lines using labelâ€free live singleâ€cell Raman spectroscopy, 2018, 49, 1323-1332.	1.2	32
64	Energy Storage: Confined Assembly of Hollow Carbon Spheres in Carbonaceous Nanotube: A Spheres-in-Tube Carbon Nanostructure with Hierarchical Porosity for High-Performance Supercapacitor (Small 19/2018). Small, 2018, 14, 1870089.	5.2	10
65	Characterisation of Liposome-Loaded Microbubble Populations for Subharmonic Imaging. Ultrasound in Medicine and Biology, 2017, 43, 346-356.	0.7	29
66	Micrometre and nanometre scale patterning of binary polymer brushes, supported lipid bilayers and proteins. Chemical Science, 2017, 8, 4517-4526.	3.7	20
67	Evaluation of lipid-stabilised tripropionin nanodroplets as a delivery route for combretastatin A4. International Journal of Pharmaceutics, 2017, 526, 547-555.	2.6	13
68	Soft Ultraviolet (UV) Photopatterning and Metallization of Self-Assembled Monolayers (SAMs) Formed from the Lipoic Acid Ester of I±-Hydroxy-1-acetylpyrene: The Generality of Acid-Catalyzed Removal of Thiol-on-Gold SAMs using Soft UV Light. ACS Applied Materials & Interfaces, 2017, 9, 18388-18397.	4.0	6
69	Simple, Direct Routes to Polymer Brush Traps and Nanostructures for Studies of Diffusional Transport in Supported Lipid Bilayers. Langmuir, 2017, 33, 3672-3679.	1.6	4
70	Controlling transmembrane protein concentration and orientation in supported lipid bilayers. Chemical Communications, 2017, 53, 4250-4253.	2.2	13
71	Plasmonic band-edge modulated surface-enhanced Raman scattering. Applied Physics Letters, 2017, 111, 051601.	1.5	4
72	Kinetically controlled fabrication of gold nanorods and investigation of their thermal stability via in-situ TEM heating. Journal of Physics: Conference Series, 2017, 902, 012007.	0.3	1

#	Article	IF	CITATIONS
73	Fluctuating Lipid Nanodomains Near Critical Transitions. Biophysical Journal, 2016, 110, 571a.	0.2	2
74	Highly Fluorescent Ribonuclease-A-Encapsulated Lead Sulfide Quantum Dots for Ultrasensitive Fluorescence <i>in Vivo</i> Imaging in the Second Near-Infrared Window. Chemistry of Materials, 2016, 28, 3041-3050.	3.2	123
75	Phospholipid dependent mechanism of smp24, an α-helical antimicrobial peptide from scorpion venom. Biochimica Et Biophysica Acta - Biomembranes, 2016, 1858, 2737-2744.	1.4	27
76	Observation of compositional domains within individual copper indium sulfide quantum dots. Nanoscale, 2016, 8, 16157-16161.	2.8	10
77	The influence of intercalating perfluorohexane into lipid shells on nano and microbubble stability. Soft Matter, 2016, 12, 7223-7230.	1.2	36
78	One-step fabrication of hollow-channel gold nanoflowers with excellent catalytic performance and large single-particle SERS activity. Nanoscale, 2016, 8, 14932-14942.	2.8	38
79	On-chip preparation of nanoscale contrast agents towards high-resolution ultrasound imaging. Lab on A Chip, 2016, 16, 679-687.	3.1	61
80	Photosynthetic Proteins in Supported Lipid Bilayers: Towards a Biokleptic Approach for Energy Capture. Small, 2015, 11, 3306-3318.	5.2	8
81	Bead-like structures and self-assembled monolayers from 2,6-dipyrazolylpyridines and their iron(<scp>ii</scp>) complexes. Journal of Materials Chemistry C, 2015, 3, 7890-7896.	2.7	25
82	Generalized circuit model for coupled plasmonic systems. Optics Express, 2015, 23, 33255.	1.7	62
83	Engineering Gold Nanotubes with Controlled Length and Nearâ€Infrared Absorption for Theranostic Applications. Advanced Functional Materials, 2015, 25, 2117-2127.	7.8	74
84	Facile Formation of Highly Mobile Supported Lipid Bilayers on Surface-Quaternized pH-Responsive Polymer Brushes. Macromolecules, 2015, 48, 3095-3103.	2.2	25
85	New Poly(amino acid methacrylate) Brush Supports the Formation of Well-Defined Lipid Membranes. Langmuir, 2015, 31, 3668-3677.	1.6	16
86	Theranostics: Engineering Gold Nanotubes with Controlled Length and Nearâ€Infrared Absorption for Theranostic Applications (Adv. Funct. Mater. 14/2015). Advanced Functional Materials, 2015, 25, 2204-2204.	7.8	1
87	Optimization of Brownian ratchets for the manipulation of charged components within supported lipid bilayers. Applied Physics Letters, 2015, 106, .	1.5	22
88	Nanooptics of Molecular-Shunted Plasmonic Nanojunctions. Nano Letters, 2015, 15, 669-674.	4.5	162
89	Self-assembly of actin scaffolds on lipid microbubbles. Soft Matter, 2014, 10, 694-700.	1.2	9
90	Reversible metallisation of soft UV patterned substrates. Journal of Materials Chemistry C, 2014, 2, 5916-5923.	2.7	4

#	Article	IF	CITATIONS
91	Poly(ethylene glycol) Lipid-Shelled Microbubbles: Abundance, Stability, and Mechanical Properties. Langmuir, 2014, 30, 5557-5563.	1.6	48
92	Enhanced Oxygen-Tolerance of the Full Heterotrimeric Membrane-Bound [NiFe]-Hydrogenase of <i>Ralstonia eutropha</i> . Journal of the American Chemical Society, 2014, 136, 8512-8515.	6.6	41
93	Diffusion in Low-Dimensional Lipid Membranes. Nano Letters, 2014, 14, 5984-5988.	4.5	15
94	Watching individual molecules flex within lipid membranes using SERS. Scientific Reports, 2014, 4, 5940.	1.6	48
95	Protein–Protein Interaction Regulates the Direction of Catalysis and Electron Transfer in a Redox Enzyme Complex. Journal of the American Chemical Society, 2013, 135, 10550-10556.	6.6	68
96	Increasing the sonoporation efficiency of targeted polydisperse microbubble populations using chirp excitation. IEEE Transactions on Ultrasonics, Ferroelectrics, and Frequency Control, 2013, 60, 2511-2520.	1.7	27
97	Fabrication and characterization of gold nano-wires templated on virus-like arrays of tobacco mosaic virus coat proteins. Nanotechnology, 2013, 24, 025605.	1.3	46
98	Alignment of a Columnar Hexagonal Discotic Liquid Crystal on Self-Assembled Monolayers. Journal of Physical Chemistry C, 2013, 117, 7533-7539.	1.5	26
99	Actin Assembly at Model-Supported Lipid Bilayers. Biophysical Journal, 2013, 105, 2355-2365.	0.2	14
100	Oxidation of Tertiary Amine-Derivatized Surfaces To Control Protein Adhesion. Langmuir, 2013, 29, 2961-2970.	1.6	12
101	Nanomechanics of Lipid Encapsulated Microbubbles with Functional Coatings. Langmuir, 2013, 29, 4096-4103.	1.6	36
102	Controlled Planar Alignment of Discotic Liquid Crystals in Microchannels Made Using SU8 Photoresist. Advanced Functional Materials, 2013, 23, 5997-6006.	7.8	34
103	Research Spotlight: Microbubbles for therapeutic delivery. Therapeutic Delivery, 2013, 4, 539-542.	1.2	9
104	High-frequency subharmonic imaging of liposome-loaded microbubbles. , 2013, , .		2
105	Liquid Crystals: Controlled Planar Alignment of Discotic Liquid Crystals in Microchannels Made Using SU8 Photoresist (Adv. Funct. Mater. 48/2013). Advanced Functional Materials, 2013, 23, 6108-6108.	7.8	0
106	Quantitation of MRI sensitivity to Quasiâ€monodisperse microbubble contrast agents for spatially resolved manometry. Magnetic Resonance in Medicine, 2013, 70, 1409-1418.	1.9	1
107	Acousto-microfluidics: Transporting microbubble and microparticle arrays in acoustic traps using surface acoustic waves. Journal of Applied Physics, 2012, 111, .	1.1	27
108	Chirp excitation of polydisperse microbubble populations for increasing sonoporation efficiency. , 2012, , .		1

#	Article	IF	CITATIONS
109	Separating the second harmonic response of tissue and microbubbles using bispectral analysis. , 2012, , .		4
110	Acousto-microfluidics: Trapping and transporting microbubbles using surface acoustic waves. , 2012, , \cdot		0
111	Manipulation and sorting of membrane proteins using patterned diffusion-aided ratchets with AC fields in supported lipid bilayers. Soft Matter, 2012, 8, 5459.	1.2	19
112	Alignment of Discotic Lyotropic Liquid Crystals at Hydrophobic and Hydrophilic Self-Assembled Monolayers. Journal of Physical Chemistry C, 2012, 116, 12627-12635.	1.5	19
113	On-Chip Alternating Current Electrophoresis in Supported Lipid Bilayer Membranes. Analytical Chemistry, 2012, 84, 10702-10707.	3.2	13
114	Temperature dependent stiffness and visco-elastic behaviour of lipid coated microbubbles using atomic force microscopy. Soft Matter, 2012, 8, 1321-1326.	1.2	26
115	Expanding 3D geometry for enhanced on-chip microbubble production and single step formation of liposome modified microbubbles. Lab on A Chip, 2012, 12, 4544.	3.1	80
116	Biotemplated Magnetic Nanoparticle Arrays. Small, 2012, 8, 204-208.	5.2	66
117	Nanoparticle Arrays: Biotemplated Magnetic Nanoparticle Arrays (Small 2/2012). Small, 2012, 8, 203-203.	5.2	1
118	Fabrication of Lipid Tubules with Embedded Quantum Dots by Membrane Tubulation Protein. Small, 2012, 8, 1590-1595.	5.2	15
119	Exploiting additive and subtractive patterning for spatially controlled and robust bacterial co-cultures. Soft Matter, 2012, 8, 9147.	1.2	8
120	Determining the Concentration of CuInS ₂ Quantum Dots from the Size-Dependent Molar Extinction Coefficient. Chemistry of Materials, 2012, 24, 2064-2070.	3.2	128
121	Driving bioenergetic processes with electrodes. Soft Matter, 2011, 7, 49-52.	1.2	6
122	Early Stages of Crystallization of Calcium Carbonate Revealed in Picoliter Droplets. Journal of the American Chemical Society, 2011, 133, 5210-5213.	6.6	105
123	Concentrating Membrane Proteins Using Asymmetric Traps and AC Electric Fields. Journal of the American Chemical Society, 2011, 133, 6521-6524.	6.6	36
124	Orientational Control over Nitrite Reductase on Modified Gold Electrode and Its Effects on the Interfacial Electron Transfer. Journal of Physical Chemistry B, 2011, 115, 12607-12614.	1.2	25
125	Spectroelectrochemical Investigation of Intramolecular and Interfacial Electron-Transfer Rates Reveals Differences Between Nitrite Reductase at Rest and During Turnover. Journal of the American Chemical Society, 2011, 133, 15085-15093.	6.6	39
126	Vesicle-modified electrodes to study proton-pumping by membrane proteins. Electrochimica Acta, 2011, 56, 10398-10405.	2.6	1

#	Article	IF	CITATIONS
127	Synthesis of nitrilotriacetic acid terminated tethers for the binding of His-tagged proteins to lipid bilayers and to gold. Tetrahedron, 2011, 67, 6246-6251.	1.0	0
128	Characteristics and durability of fluoropolymer thin films. Polymer Degradation and Stability, 2011, 96, 561-565.	2.7	7
129	The periodicity between the aggregated microbubbles by secondary radiation force. , 2011, , .		2
130	Cholesterol-based anchors and tethers for phospholipid bilayers and for model biological membranes. Soft Matter, 2010, 6, 6036.	1.2	39
131	A study of cytochrome bo3 in a tethered bilayer lipid membrane. Biochimica Et Biophysica Acta - Bioenergetics, 2010, 1797, 1917-1923.	0.5	20
132	A Selfâ€assembly Route for Double Bilayer Lipid Membrane Formation. ChemPhysChem, 2010, 11, 569-574.	1.0	21
133	Effect of the Structure of Cholesterolâ€Based Tethered Bilayer Lipid Membranes on Ionophore Activity. ChemPhysChem, 2010, 11, 2191-2198.	1.0	32
134	Planar Alignment of Columnar Discotic Liquid Crystals by Isotropic Phase Dewetting on Chemically Patterned Surfaces. Advanced Functional Materials, 2010, 20, 914-920.	7.8	42
135	Synthesis of High‣urfaceâ€Area Platinum Nanotubes Using a Viral Template. Advanced Functional Materials, 2010, 20, 1295-1300.	7.8	118
136	Nearâ€Bulk Conductivity of Gold Nanowires as Nanoscale Interconnects and the Role of Atomically Smooth Interface. Advanced Materials, 2010, 22, 2338-2342.	11.1	106
137	Controlling Liquid Crystal Alignment Using Photocleavable Cyanobiphenyl Self-Assembled Monolayers. ACS Applied Materials & Interfaces, 2010, 2, 3686-3692.	4.0	29
138	Force spectroscopy of streptavidin conjugated lipid coated microbubbles. Bubble Science, Engineering & Technology, 2010, 2, 48-54.	0.2	14
139	STW resonator with organo-functionalized metallic nanoparticle film for vapor sensing. IEEE Transactions on Ultrasonics, Ferroelectrics, and Frequency Control, 2009, 56, 1018-1023.	1.7	Ο
140	Formation and manipulation of two-dimensional arrays of micron-scale particles in microfluidic systems by surface acoustic waves. Applied Physics Letters, 2009, 94, .	1.5	68
141	Photoelectric Properties of Electrodeposited Copper(I) Oxide Nanowires. Journal of the Electrochemical Society, 2009, 156, K191.	1.3	13
142	A Cholesterolâ€Based Tether for Creating Photopatterned Lipid Membrane Arrays on both a Silica and Gold Surface. Chemistry - A European Journal, 2009, 15, 6363-6370.	1.7	19
143	The adhesive properties of pyridine-terminated self-assembled monolayers. Thin Solid Films, 2009, 517, 3806-3812.	0.8	3
144	Surface Plasmon Raman Scattering Studies of Liquid Crystal Anchoring on Liquid-Crystal-Based Self-Assembled Monolayers. Journal of Physical Chemistry B, 2009, 113, 15550-15557.	1.2	10

#	Article	IF	CITATIONS
145	Improved Photoreaction Yields for Soft Ultraviolet Photolithography in Organothiol Self-Assembled Monolayers. Journal of Physical Chemistry C, 2009, 113, 21642-21647.	1.5	26
146	Anomalous uniform domain in a twisted nematic cell constructed from micropatterned surfaces. Liquid Crystals, 2009, 36, 353-358.	0.9	7
147	Manipulation and charge determination of proteins in photopatterned solid supported bilayers. Integrative Biology (United Kingdom), 2009, 1, 205-211.	0.6	37
148	Characterization of cytochrome <i>bo</i> 3 activity in a native-like surface-tethered membrane. Biochemical Journal, 2009, 417, 555-560.	1.7	25
149	In vitro biosynthesis of bacterial peptidoglycan using d-Cys-containing precursors: fluorescent detection of transglycosylation and transpeptidation. Chemical Communications, 2009, , 4037.	2.2	3
150	pH-dependent adsorption of Au nanoparticles on chemically modified Si ₃ N ₄ MEMS devices. Journal of Experimental Nanoscience, 2009, 4, 147-157.	1.3	4
151	Vapour phase formation of amino functionalised Si3N4 surfaces. Surface Science, 2008, 602, 2724-2733.	0.8	10
152	The pH-dependent adhesion of nanoparticles to self-assembled monolayers on gold. Thin Solid Films, 2008, 516, 2987-2999.	0.8	9
153	Impedance Spectroscopy of Bacterial Membranes: Coenzyme-Q Diffusion in a Finite Diffusion Layer. Analytical Chemistry, 2008, 80, 9084-9090.	3.2	11
154	Native <i>E. coli</i> inner membrane incorporation in solid-supported lipid bilayer membranes. Biointerphases, 2008, 3, FA59-FA67.	0.6	39
155	Minimal F-Actin Cytoskeletal System for Planar Supported Phospholipid Bilayers. Langmuir, 2008, 24, 6827-6836.	1.6	33
156	Self-Assembled Layers Based on Isomerizable Stilbene and Diketoarylhydrazone Moieties. Langmuir, 2008, 24, 2479-2486.	1.6	20
157	Chemical Manipulation by X-rays of Functionalized Thiolate Self-Assembled Monolayers on Au. Langmuir, 2008, 24, 13969-13976.	1.6	31
158	Four-probe electrical characterization of Pt-coated TMV-based nanostructures. Nanotechnology, 2008, 19, 165704.	1.3	32
159	A 106-fold enhancement in the conductivity of a discotic liquid crystal doped with only 1% (wâ^•w) gold nanoparticles. Journal of Applied Physics, 2008, 103, .	1.1	54
160	Magnetic field enhanced nano-tip fabrication for four-probe STM studies. Nanotechnology, 2008, 19, 085201.	1.3	11
161	Alignment of particles in microfluidic systems using standing surface acoustic waves. Applied Physics Letters, 2008, 92, .	1.5	89
162	Site-Directed Conjugation of "Clicked―Glycopolymers To Form Glycoprotein Mimics:  Binding to Mammalian Lectin and Induction of Immunological Function. Journal of the American Chemical Society, 2007, 129, 15156-15163.	6.6	281

#	Article	IF	CITATIONS
163	Nematic liquid crystal alignment on chemical patterns. Liquid Crystals, 2007, 34, 1059-1069.	0.9	37
164	A Model System To Study the Insertion of Cholesterol into a Phospholipid Monolayer. Journal of Physical Chemistry B, 2007, 111, 379-386.	1.2	15
165	Photo-deprotection patterning of self-assembled monolayers. Journal of Experimental Nanoscience, 2007, 2, 279-290.	1.3	6
166	Titration of Ionizable Monolayers by Measurement of the Electric Double-Layer Force. Langmuir, 2007, 23, 6893-6895.	1.6	7
167	A Novel Method To Fabricate Patterned Bilayer Lipid Membranes. Langmuir, 2007, 23, 1354-1358.	1.6	30
168	Four-probe electrical transport measurements on individual metallic nanowires. Nanotechnology, 2007, 18, 065204.	1.3	71
169	Fabrication of a nanoparticle gradient substrate by thermochemical manipulation of an ester functionalized SAM. Journal of Materials Chemistry, 2007, 17, 5097.	6.7	13
170	Tethered Bilayer Lipid Membranes Studied by Simultaneous Attenuated Total Reflectance Infrared Spectroscopy and Electrochemical Impedance Spectroscopy. Journal of Physical Chemistry B, 2007, 111, 3515-3524.	1.2	30
171	Supported Bilayer Lipid Membrane Arrays on Photopatterned Selfâ€Assembled Monolayers. Chemistry - A European Journal, 2007, 13, 7957-7964.	1.7	36
172	Proton transport into a tethered bilayer lipid membrane. Electrochemistry Communications, 2007, 9, 610-614.	2.3	32
173	Phase separation in mixed self-assembled monolayers and its effect on biomimetic membranes. Sensors and Actuators B: Chemical, 2007, 124, 501-509.	4.0	67
174	Comparative characterisation by atomic force microscopy and ellipsometry of soft and solid thin films. Surface and Interface Analysis, 2007, 39, 575-581.	0.8	20
175	Novel 3,4-disubstituted thiophenes for weak passivation of Au nanoparticles. Journal of Experimental Nanoscience, 2006, 1, 143-164.	1.3	3
176	Surfactant mediated assembly of gold nanowires on surfaces. Journal of Experimental Nanoscience, 2006, 1, 125-142.	1.3	15
177	Self-Assembly of Actin Scaffolds at Ponticulin-Containing Supported Phospholipid Bilayers. Biophysical Journal, 2006, 90, L21-L23.	0.2	13
178	Redox Enzymes in Tethered Membranes. Journal of the American Chemical Society, 2006, 128, 1711-1716.	6.6	127
179	pH-Dependent gold nanoparticle self-organization on functionalized Si/SiO2surfaces. Journal of Experimental Nanoscience, 2006, 1, 333-353.	1.3	31
180	Soft-UV Photolithography using Self-Assembled Monolayers. Journal of Physical Chemistry B, 2006, 110, 17167-17174.	1.2	35

#	Article	IF	CITATIONS
181	Fabrication of Gold Micro- and Nanostructures by Photolithographic Exposure of Thiol-Stabilized Gold Nanoparticles. Nano Letters, 2006, 6, 345-350.	4.5	77
182	Fabrication of Biological Nanostructures by Scanning Near-Field Photolithography of Chloromethylphenylsiloxane Monolayers. Nano Letters, 2006, 6, 29-33.	4.5	75
183	Multilayers of 4-methylbenzenethiol functionalized gold nanoparticles fabricated by Langmuir–Blodgett and Langmuir–Schaefer deposition. Colloids and Surfaces A: Physicochemical and Engineering Aspects, 2006, 278, 98-105.	2.3	23
184	Antibiotic Action and Peptidoglycan Formation on Tethered Lipid Bilayer Membranes. Angewandte Chemie - International Edition, 2006, 45, 2111-2116.	7.2	37
185	Dielectrophoretic manipulation and electrical characterization of gold nanowires. Nanotechnology, 2005, 16, 1500-1505.	1.3	112
186	A Mild Photoactivated Hydrophilic/Hydrophobic Switch. Langmuir, 2005, 21, 4554-4561.	1.6	48
187	Novel cyanoterphenyl self-assembly monolayers on Au(111) studied by ellipsometry, x-ray photoelectron spectroscopy, and vibrational spectroscopies. Journal of Chemical Physics, 2005, 122, 224707.	1.2	11
188	Ellipsometric study of adsorption on nanopatterned block copolymer substrates. Journal of Chemical Physics, 2005, 122, 104902.	1.2	3
189	Direct Electrochemical Interaction between a Modified Gold Electrode and a Bacterial Membrane Extract. Langmuir, 2005, 21, 1481-1488.	1.6	50
190	Photooxidation of Self-Assembled Monolayers by Exposure to Light of Wavelength 254 nm:Â A Static SIMS Study. Journal of Physical Chemistry B, 2005, 109, 11247-11256.	1.2	72
191	Ordered structures and phase transitions in thin films of polystyrene/polyisoprene block copolymer and blends with the corresponding homopolymers. Journal of Materials Science, 2004, 39, 2249-2252.	1.7	8
192	Gold Nanoparticle Patterning of Silicon Wafers Using Chemical e-Beam Lithography. Langmuir, 2004, 20, 3766-3768.	1.6	203
193	A Novel Example of X-Ray-Radiation-Induced Chemical Reduction of an Aromatic Nitro-Group-Containing Thin Film on SiO2 to an Aromatic Amine Film. ChemPhysChem, 2003, 4, 884-889.	1.0	82
194	Spectroscopic Ellipsometric Evaluation of Gold Nanoparticle Thin Films Fabricated Using Layer-by-Layer Self-Assembly. Advanced Materials, 2003, 15, 531-534.	11.1	44
195	Surface energy of ethylene-co-1-butene copolymers determined by contact angle methods. Journal of Colloid and Interface Science, 2003, 260, 234-239.	5.0	23
196	Surface functionalisation for the self-assembly of nanoparticle/polymer multilayer films. Thin Solid Films, 2003, 426, 31-39.	0.8	52
197	Electronic properties of hybrid metal-discotic liquid crystal nanostructures. Physica E: Low-Dimensional Systems and Nanostructures, 2003, 17, 654-658.	1.3	3
198	Fabrication and Characterization of Self-Assembled Nanoparticle/Polyelectrolyte Multilayer Films. Journal of Physical Chemistry B, 2003, 107, 13557-13562.	1.2	30

#	Article	IF	CITATIONS
199	Spectroscopic Characterization of Gold Nanoparticles Passivated by Mercaptopyridine and Mercaptopyrimidine Derivatives. Journal of Physical Chemistry B, 2003, 107, 6087-6095.	1.2	74
200	The p7 protein of hepatitis C virus forms an ion channel that is blocked by the antiviral drug, Amantadine. FEBS Letters, 2003, 535, 34-38.	1.3	403
201	Hybrid silicon–organic nanoparticle memory device. Journal of Applied Physics, 2003, 94, 5234.	1.1	96
202	Anchoring and orientational wetting of nematic liquid crystals on semi-fluorinated self-assembled monolayer surfaces. Europhysics Letters, 2002, 59, 410-416.	0.7	27
203	Quantum interference effects in nanostructured Au. Journal of Physics Condensed Matter, 2002, 14, 11779-11783.	0.7	0
204	Interactions of self-organised discotic liquid crystals with ultrathin metal films. Materials Science and Technology, 2002, 18, 729-732.	0.8	1
205	Lipid Vesicle Fusion on μCP Patterned Self-Assembled Monolayers: Effect of Pattern Geometry on Bilayer Formation. Langmuir, 2002, 18, 3176-3180.	1.6	57
206	A Biomimetic Membrane Consisting of a Polyethyleneoxythiol Monolayer Anchored to Mercury with a Phospholipid Bilayer on Top. Journal of Physical Chemistry B, 2002, 106, 10410-10416.	1.2	35
207	Magnetic Resonance Imaging of Strawberry (Fragaria vesca) Slices During Osmotic Dehydration and Air Drying. LWT - Food Science and Technology, 2002, 35, 177-184.	2.5	24
208	Vapour sensing using surface functionalized gold nanoparticles. Nanotechnology, 2002, 13, 439-444.	1.3	111
209	Enhanced charge conduction in discotic liquid crystals. Journal of Materials Chemistry, 2001, 11, 1982-1984.	6.7	19
210	Single Ion Channel Sensitivity in Suspended Bilayers on Micromachined Supports. Langmuir, 2001, 17, 1240-1242.	1.6	68
211	Polymerization of Semi-Fluorinated Alkane Thiol Self-Assembled Monolayers Containing Diacetylene Units. Langmuir, 2001, 17, 6616-6621.	1.6	21
212	<title>Lipid bilayers suspended on microfabricated supports</title> ., 2001, , .		1
213	Synthesis of novel biotin anchors. Tetrahedron, 2001, 57, 9859-9866.	1.0	22
214	Room-temperature single-electron tunnelling in surfactant stabilised iron oxide nanoparticles. Physica E: Low-Dimensional Systems and Nanostructures, 2001, 9, 253-261.	1.3	41
215	Title is missing!. Cellulose, 2001, 8, 297-301.	2.4	2
216	Wetting transitions of simple liquid films adsorbed on self-assembled monolayer substrates: an ellipsometric study. Molecular Physics, 2000, 98, 807-814.	0.8	3

#	Article	IF	CITATIONS
217	Detection of complement activity by using a polysaccharide-protected membrane. Enzyme and Microbial Technology, 2000, 26, 301-303.	1.6	6
218	Conductivity of two-dimensional metal–organic hybrid films. Microelectronic Engineering, 2000, 51-52, 633-644.	1.1	2
219	Discrete membrane arrays. Reviews in Molecular Biotechnology, 2000, 74, 159-174.	2.9	26
220	Vapour sensing using hybrid organic–inorganic nanostructured materials. Journal of Materials Chemistry, 2000, 10, 183-188.	6.7	202
221	Suspended Planar Phospholipid Bilayers on Micromachined Supports. Langmuir, 2000, 16, 5696-5701.	1.6	41
222	Wetting transitions of simple liquid films adsorbed on selfassembled monolayer substrates: an ellipsometric study. Molecular Physics, 2000, 98, 807-814.	0.8	1
223	Microcontact Printing of Lipophilic Self-Assembled Monolayers for the Attachment of Biomimetic Lipid Bilayers to Surfaces. Journal of the American Chemical Society, 1999, 121, 5274-5280.	6.6	104
224	Triphenylene-Based Discotic Liquid Crystals as Self-Assembled Monolayers. Langmuir, 1999, 15, 3790-3797.	1.6	56
225	Use of Mixed Self-Assembled Monolayers in a Study of the Effect of the Microenvironment on Immobilized Glucose Oxidase. Langmuir, 1999, 15, 1198-1207.	1.6	86
226	N,N′-Disuccinimidyl carbonate as a coupling agent in the synthesis of thiophospholipids used for anchoring biomembranes to gold surfaces. Tetrahedron, 1998, 54, 11537-11548.	1.0	27
227	Ion-Selective Lipid Bilayers Tethered to Microcontact Printed Self-Assembled Monolayers Containing Cholesterol Derivatives. Langmuir, 1998, 14, 4675-4678.	1.6	61
228	Attenuated Total Reflection Fourier Transform Infrared Spectroscopic Characterization of Fluid Lipid Bilayers Tethered to Solid Supports. Langmuir, 1998, 14, 839-844.	1.6	54
229	High-resolution inverted x-ray photoelectron diffraction studies of Si(100). Journal of Physics Condensed Matter, 1997, 9, 1967-1982.	0.7	3
230	Kinetics of the Unrolling of Small Unilamellar Phospholipid Vesicles onto Self-Assembled Monolayers. Langmuir, 1997, 13, 751-757.	1.6	160
231	X-ray photoelectron spectroscopy of partial and stamped thiol-based self-assembled monolayers. Supramolecular Science, 1997, 4, 247-253.	0.7	8
232	Immobilization of glucose oxidase onto a Langmuir-Blodgett ultrathin film of a cellulose derivative deposited on a self-assembled monolayer. Supramolecular Science, 1997, 4, 279-291.	0.7	22
233	Kinetics of formation of single phospholipid bilayers on self-assembled monolayer supports, as monitored by surface plasmon resonance. Supramolecular Science, 1997, 4, 513-517.	0.7	29
234	Synthesis and characterisation of surfactant-stabilised gold nanoparticles. Supramolecular Science, 1997, 4, 329-333.	0.7	17

#	Article	IF	CITATIONS
235	The design and synthesis of simple molecular tethers for binding biomembranes to a gold surface. Tetrahedron, 1997, 53, 10939-10952.	1.0	83
236	Correction for the effects of adventitious carbon overlayers in quantitative XPS analysis. Surface and Interface Analysis, 1997, 25, 924-930.	0.8	60
237	Surface-field induced organisation at solid/fluid interfaces. Faraday Discussions, 1996, 104, 37.	1.6	21
238	A combined in situ optical reflectance–electron diffraction study of Co/Cu and Co/Au multilayers grown by molecular beam epitaxy. Applied Physics Letters, 1996, 68, 3740-3742.	1.5	7
239	Inverted photoelectron diffraction: a new technique for surface structure determination. Journal of Electron Spectroscopy and Related Phenomena, 1995, 70, 217-223.	0.8	5
240	XPS Studies of Self-Assembled Multilayer Films. Langmuir, 1995, 11, 4411-4417.	1.6	71
241	Self-Assembled Multilayer Formation on Predefined Templates. Langmuir, 1995, 11, 3811-3814.	1.6	29
242	Mixed alkanethiolate monolayers as substrates for studying the Langmuir film deposition process. Thin Solid Films, 1994, 243, 325-329.	0.8	15
243	Raman spectroscopy of self-assembled mono- and multilayer films of alkanethiolate on gold. Thin Solid Films, 1994, 244, 778-783.	0.8	25
244	Multilayers of ω-mercaptoalkanoic acids containing a polar aromatic group: characterization of films. Thin Solid Films, 1994, 244, 784-788.	0.8	26
245	Self-Assembled Monolayers containing Polydiacetylenes. Journal of the American Chemical Society, 1994, 116, 1050-1053.	6.6	172
246	Mixed alkanethiol monolayers on gold surfaces: substrates for Langmuir-Blodgett film deposition. Langmuir, 1993, 9, 1024-1027.	1.6	21
247	Estimation of the uncertainties associated with XPS peak intensity determination. Surface and Interface Analysis, 1992, 18, 323-332.	0.8	28
248	Surface potentials of Langmuir-Blodgett alternating layer structures. Thin Solid Films, 1992, 210-211, 4-5.	0.8	10
249	Self-assembled monolayers of alkanethiols on gold: sulfone groups enhancing two-dimensional organization. Thin Solid Films, 1992, 210-211, 806-809.	0.8	6
250	Wetting studies of molecularly heterogeneous surfaces using two liquid systems. Thin Solid Films, 1992, 210-211, 810-814.	0.8	7
251	Mixed alkanethiol monolayers on gold surfaces: Wetting and stability studies. Advances in Colloid and Interface Science, 1992, 39, 175-224.	7.0	52
252	Concentration-driven surface transition in the wetting of mixed alkanethiol monolayers on gold. Journal of the American Chemical Society, 1991, 113, 1499-1506.	6.6	171

#	Article	IF	CITATIONS
253	Self-assembled multilayers of .omegamercaptoalkanoic acids: selective ionic interactions. Journal of the American Chemical Society, 1991, 113, 5866-5868.	6.6	163
254	Monolayers having large in-plane dipole moments: characterization of sulfone-containing self-assembled monolayers of alkanethiols on gold by Fourier transform infrared spectroscopy, x-ray photoelectron spectroscopy and wetting. Langmuir, 1991, 7, 2700-2709.	1.6	79
255	Contact angle stability: Reorganization of monolayer surfaces?. Langmuir, 1991, 7, 156-161.	1.6	155
256	Self-assembled monolayers of alkanethiols containing a polar aromatic group: effects of the dipole position on molecular packing, orientation, and surface wetting properties. Journal of the American Chemical Society, 1991, 113, 4121-4131.	6.6	195
257	Curve synthesis and optimization procedures for X-ray photoelectron spectroscopy. Surface and Interface Analysis, 1991, 17, 85-93.	0.8	46
258	Surface potential studies of alkyl-thiol monolayers adsorbed on gold. Chemical Physics Letters, 1990, 170, 462-466.	1.2	240
259	Structural and electrical studies of alternating layers of porphyrins and fatty acids. Thin Solid Films, 1988, 160, 99-105.	0.8	24
260	Langmuir—Blodgett films from porphyrins. British Polymer Journal, 1987, 19, 397-400.	0.7	6
261	Angular dependence of X-ray-excited valence-band photoelectron spectra of diamond. Journal of the Chemical Society, Faraday Transactions 2, 1986, 82, 541.	1.1	16
262	Convolutional smoothing algorithms in electron spectroscopy. Surface and Interface Analysis, 1986, 8, 71-73.	0.8	15
263	Interfacing AEI/Kratos electron spectrometers to a microcomputer for data acquisition and processing. Surface and Interface Analysis, 1982, 4, 267-270.	0.8	12
264	Relative differential subshell photoionisation cross-sections (MgKα) from lithium to uranium. Journal of Electron Spectroscopy and Related Phenomena, 1978, 14, 341-358.	0.8	177
265	Quantitative analysis of aluminosilicates and other solids by x-ray photoelectron spectroscopy. Analytical Chemistry, 1977, 49, 2001-2008.	3.2	66
266	Oxidation of the group IBmetals studied by X-ray and ultraviolet photoelectron spectroscopy. Part 1.—The surface oxidation of polycrystalline copper. Journal of the Chemical Society, Faraday Transactions 2, 1975, 71, 1044-1057.	1.1	67
267	Determination of relative electron inelastic mean free paths (escape depths) and photoionisation cross-sections by X-ray photoelectron spectroscopy. Journal of the Chemical Society, Faraday Transactions 2, 1975, 71, 1777.	1.1	32
268	A multi-stack insulator silicon-organic memory device with gold nanoparticles. , 0, , .		0
269	Nanomagnetic Arrays Formed with the Biomineralization Protein Mms6. Journal of Nano Research, O, 17, 127-146.	0.8	18
270	Targeting Tumour Vasculature using Integrin αvβ3 - Observation of Liposome Accumulation in Microfluidic Vasculature Networks. , 0, , .		0

#	Article	IF	CITATIONS
271	Alternating defects and egg and dart textures in de-wetted stripes of discotic liquid crystal. Liquid Crystals, 0, , 1-16.	0.9	2